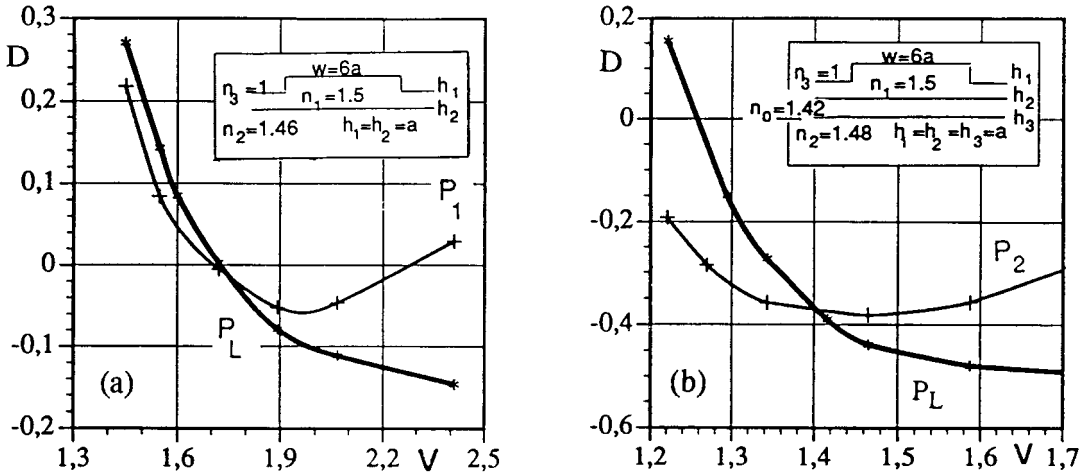

Figure 3 The waveguide dispersion term D as a function of V for a normal rib structure (a) and a depressed index rib (b) with a Kerr-like nonlinear guiding region having $n_{nL} = 0.54 \times 10^{-10}$ [m^2/V^2]. Dimension $a = 1$ μm, P_L = linear state power level (bold lines); $P_1 = 1$ μW, $P_2 = 0.8$ μW, nonlinear state power levels

in frequency. When operating at a given frequency the dispersion nonlinear values may be very different from those of the linear state, and their correct value must be evaluated starting from a nonlinear model of the structure. The indicated dispersion nonlinear behavior is presented as an example, but the analysis of other different rib structures allow us to generalize the results. Further investigation must be extended in this direction.

CONCLUSIONS

In a standard rib waveguide the change of parameters has not proved to be very effective in the control of the group velocity dispersion; in particular, no negative dispersion may be obtained in the single-mode region. When a depressed index layer (usually called a *notch*) is interposed between the guiding region and the substrate, a negative GVD may be easily obtained; in a rib guide with a proper choice of other parameters as the width of the loading strip a controlled amount of negative GVD may be obtained and the region of single-mode operation may be extended. Under high optical intensity when a Kerrlike nonlinear behavior in the guiding region must be taken into account, the waveguide dispersion must be evaluated under a nonlinear model because those nonlinear values may be very different from those of the linear state.

ACKNOWLEDGMENT

The author wish to thank Professor Lucio Manià and Prof. Edoardo Carli for their useful advice and suggestions, and for help with the graphical presentation.

REFERENCES

1. E. Valentinuzzi, "A Vectorial Finite Element Solution of Anisotropic Optical Waveguides," *Tec. Ital.*, Vol. 59, No. 4, 1994, pp. 249–254.
2. E. Valentinuzzi, "Direct Finite Element Computation of Dispersion Parameters of Optical Waveguides," *Electron. Lett.*, Vol. 30, No. 15, 1994, pp. 1217–1219.
3. S. Kawakami and S. Nishida, "Characteristics of a Doubly Clad Optical Fiber with a Low-Index Inner Cladding," *IEEE J. Quantum Electron.*, Vol. QE-10, No. 12, 1974, pp. 879–887.
4. A. Dienes, Y. Peng, and A. Knoesen, "Group Velocity Dispersion in Depressed Index Type Planar Waveguides," *Appl. Opt.*, Vol. 29, No. 12, 1990, pp. 1722–1724.

CCC 0895-2477/97

1.55-μm OPTICAL PHASE-LOCKED LOOP WITH INTEGRATED *p-i-n*/HBT PHOTORECEIVER IN A FLEXIBLE DEVELOPMENT PLATFORM

P. G. Goetz,[1] H. Eisele,[1] K. C. Syao,[1] and P. Bhattacharya[1]
[1] Solid State Electronics Laboratory
Department of Electrical Engineering and Computer Science
University of Michigan
Ann Arbor, Michigan 48109

Received 3 December 1996

ABSTRACT: *A monolithically integrated p-i-n / HBT photoreceiver was successfully employed in a development platform for hybrid optical phase-locked loops (OPLLs). Despite loop delay compromises necessary for flexibility in component substitution, this OPLL development platform has demonstrated a hold-in range of 1.558 GHz and possible locking frequencies from 1.00 to 20.75 GHz. © 1997 John Wiley & Sons, Inc.* Microwave Opt Technol Lett 15: 4–7, 1997.

Key words: *OPLL; p-i-n / HBT photoreceiver; WDM; optoelectronic circuits; optical communications*

1. INTRODUCTION

Optical phase-locked loops (OPLLs) are being developed to provide a method of generating channel offsets for use in dense wavelength-division multiplexed (WDM) systems. It is possible to maintain a stable channel separation on the order of 0.01–0.1 nm between the master and slave laser with the use of an OPLL. The offset is determined by an electronic local oscillator (LO) reference. OPLLs also show promise for use in generating highly stable microwave carriers, which can be distributed via an optical fiber network for phased array antennas. They can also be used as phase or frequency

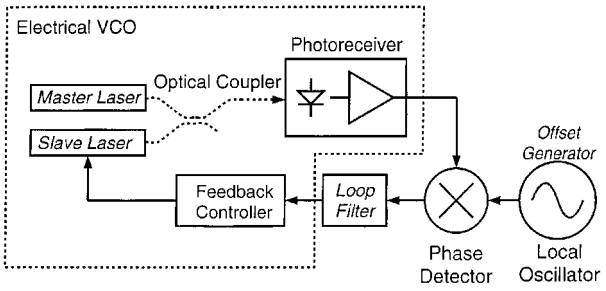

Figure 1 Schematic diagram of optical phase-locked loop

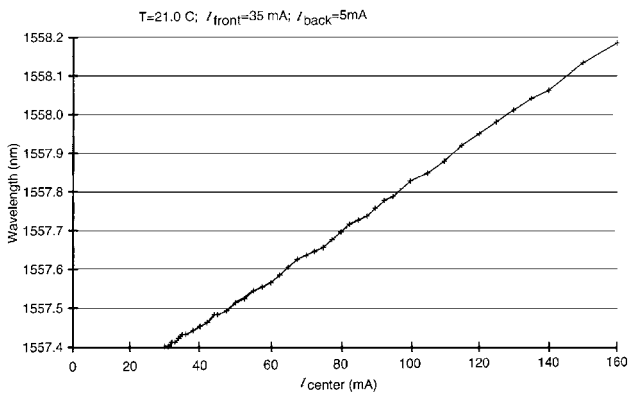

Figure 2 Typical three-section DFB current tuning characteristics. Horizontal axis I_{center} (scale 20 mA/division), vertical axis wavelength (scale 0.1 nm/division). $T = 21.0$ C, $I_{\text{front}} = 35$ mA, $I_{\text{rear}} = 5$ mA

demodulators. The development of monolithically integrated OPLLs will make their widespread application more feasible.

Typical approaches to making hybrid OPLLs use either very narrow linewidth lasers or reduce the loop delay as much as possible. The use of semiconductor lasers with their moderately large linewidths has encouraged the development of very compact but inflexible loop designs, which make the loops undesirable for component substitution and testing. Previous designs with the use of semiconductor lasers have avoided the use of fiber couplers to minimize loop delay.

A hybrid, fiber-based system allows design, layout, and testing flexibility, which is necessary in a test bed for the development of components for an integrated OPLL. In spite of the large loop delay that comes from using fiber components, we demonstrate that phase locking can be achieved with the use of semiconductor lasers of moderate linewidths and fiber components. We achieved a very wide hold-in range of 1.558 GHz and possible locking frequencies ranging from 1.00 to 20.75 GHz, both of which are among the best reported values.

As the first step toward integration, a monolithically integrated *p-i-n*/HBT photoreceiver was successfully employed in the test bed.

1.1. OPLL Operation. An OPLL is similar in construction to a conventional phase-locked loop (PLL). The electronic voltage-controlled oscillator (VCO) is replaced with an optoelectronic current controlled oscillator (CCO). When the loop is locked, the wavelength separation between the two lasers is fixed to a value specified by the LO reference oscillator.

The basic OPLL configuration can be seen in Figure 1. Two lasers are heterodyned by an optical coupler or beam splitter onto a photodetector. The beat frequency resulting from the difference in the lasers' wavelengths (and hence, the difference in frequency) is converted by the photodetector into an electrical frequency. A phase detector compares this beat frequency with the LO frequency, and the resulting error signal is fed back to the slave laser to maintain the beat frequency equal to the LO frequency.

The operation of the optoelectronic CCO is based on the dc current tuning characteristics of semiconductor lasers. Typical distributed feedback (DFB) semiconductor laser characteristics are shown in Figure 2. Operating wavelength changes with current due to both thermal and carrier effects [1]. In general, as current increases, operating wavelength increases in a DFB laser. This changes the wavelength difference between the master and slave lasers and hence the beat frequency. This optical beat frequency is detected and output as an electrical frequency. Thus the laser pair, optical coupler, and photodetector comprise an oscillator whose electrical frequency output is determined by the dc current input.

1.2. Benefits of Integration. A monolithically integrated form of the photonic circuit is a highly desirable goal for an OPLL. Because the CCOs used in OPLLs have much larger linewidths than the VCOs used in PLLs, the effect of the loop delay must be taken into account [2]. OPLLs can have large loop delays due to the optical path length and rigid placement requirements of optical components. Minimum loop delay, which is highly desirable for OPLLs used in actual communications systems, can be more easily achieved by integration of the optical and electrical components.

Further benefits of integration include the elimination of problems associated with alignment of optical components and the significant reduction in size, both of which improve the system's overall cost effectiveness. Integration also facilitates the development of and practicality of multichannel WDM systems that use OPLLs.

1.3. Previous Work Toward Integration. The first step toward integration of OPLLs was the use of semiconductor lasers. Several OPLLs have been demonstrated with semiconductor lasers, initially with external line-narrowing techniques [3], and later without [4, 5]. Other OPLL components have also been integrated, but have not yet been used in an OPLL. These include microwave monolithic integrated circuit (MMIC) phase detectors [6], optical couplers, and photoreceivers [7].

A transistor-based process is necessary in the overall integration scheme, because the local-oscillator MMIC for the reference signal, the phase detector, low noise amplifiers (LNAs), and eventually laser driver components must be realized with a high-speed transistor design. Furthermore, with the use of heterojunction bipolar transistor (HBT) technology, a *p-i-n*/HBT front-end photoreceiver can be fabricated [8, 9], and can replace the photodiode in the OPLL with a high-gain optical detection device. The base-collector–subcollector layers of the HBT serve as the *p-i-n* diode. Thus a high-speed, low-noise transistor is monolithically integrated with a high-performance photodiode.

We have recently demonstrated such photoreceiver circuits with measured modulation bandwidth $f_{-3\,\text{dB}} = 19.5$ GHz, and an estimated sensitivity of -18.7 dBm at 10 Gb/s

for a bit error rate of 10^{-9} and $\lambda = 1.55$ μm [10]. The HBTs used in this process have an f_T of 67 GHz and f_{max} of 120 GHz, and thus could be used for the MMIC components.

2. RESULTS AND DISCUSSION

In this article we describe the development of a 1.55-μm hybrid OPLL made of commercially available discrete components to serve as a flexible test bed for integrated components as they are developed. We then demonstrate the use of an InP-based *p-i-n*/HBT photoreceiver in a test bed. We show that a wide hold-in range can be obtained, and a wide frequency range for testing is possible in a fiber-based test system, in spite of the long loop delay involved.

2.1. Hybrid OPLL Test Bed Setup. As the first step toward monolithic integration, an OPLL comprised of commercially available discrete components was developed to serve as a test bed for monolithically integrated components as they are developed. The two primary competing considerations for such a design were to minimize the loop delay and to maintain a degree of flexibility in the physical setup so that different components and topologies could be tested without redesigning the loop for each new experiment.

Figure 3 shows the experimental setup of the OPLL test bed. Two temperature-stabilized 1.55-μm three-section DFB lasers (IMC, Sweden) were heterodyned with a fiber coupler onto a commercial photodiode (New Focus 1011). The electrical signal from the photodetector was amplified by two LNAs (MITEQ JS4 and AFS4 series). The summed linewidth of the free-running lasers was about 6 MHz, as measured with a spectrum analyzer. Sixty-five-decibel optical isolaters were used to avoid an increase in free-running linewidth [4]. The amplified electrical signal was compared with a reference signal from an HP 8350B sweep oscillator with the use of a double-balanced diode mixer (Norsal DBM 1-12A) as a phase detector. The phase difference signal from the mixer was fed back to the slave laser through a passive loop filter, then through a bias offset circuit to change the dc bias of the error signal to the value required for slave laser operation. A modified first-order loop filter [11] was used, as it is less sensitive to loop delay than second-order loops [12]. Connectorized fiber components were used for all optical elements to allow photodiodes or photoreceivers to be easily interchanged.

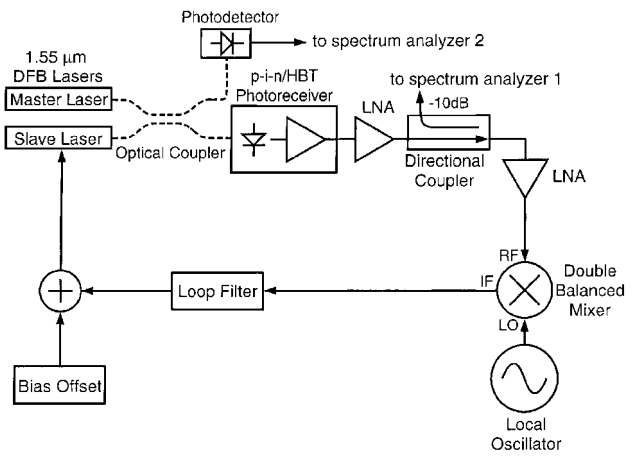

Figure 3 Experimental setup of optical phase-locked-loop test bed

Initially a −10-dB directional coupler was placed between the second LNA and the mixer. However, the LO signal was observed at spectrum analyzer 1, due to poor LO to rf isolation through the mixer. The directional coupler was then moved to the position shown in Figure 3, which removed most of the LO signal. The second output of the optical coupler was heterodyned onto a separate photodetector (Picometrix D-15), to electrically isolate the reference oscillator from the spectrum analyzer. Both spectrum analyzers were used throughout the experiment to monitor the spectrum both within and outside of the loop.

2.2. Hybrid OPLL Test Bed Experiments. Figure 4 shows the spectrum of the beat signal when locking is achieved as measured by the electrically isolated photodetector. Total LNA gain was approximately 60 dB. The delay of the electronic components and connectors was measured with an HP 8510B network analyzer to be 1.9 ns. This could be reduced to less than 1 ns with the removal of the directional coupler and one LNA. The optical path delay was estimated by its length to be 2.4 ns. In spite of this very large loop delay due mainly to the use of fibers, continuous locking from 3.820 to 5.378 GHz was obtained, which corresponds to an excellent hold-in range of 1.558 GHz. The beat signal under phase-locked conditions was monitored for over 1 h with the control voltage at the slave laser indicating a large margin of safety throughout the time. Fluctuations of the control voltage over that period of time were less than 20% of the total range. Therefore, we believe the lock could have been maintained over a much longer period of time if desired.

Subsequently, an amplifier with a wider bandwidth but lower gain (total LNA gain now approximately 54 dB) was substituted, and the new circuit was phase locked at various beat frequencies in a very large continuous range between 1.00 and 20.75 GHz. With the master laser wavelength tuned to 1556.98 nm, this corresponds to the ability to lock the slave laser wavelength anywhere between 1556.99 and 1557.15 nm. To the best of our knowledge, this represents both the largest

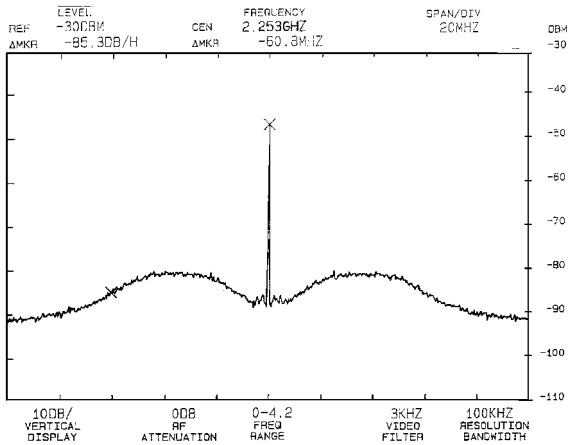

Figure 4 Spectrum of beat signal under phase-lock conditions as measured by spectrum analyzer 2. Center frequency 2.253 GHz, vertical scale 10 dB/division, horizontal scale 20 MHz/division, video filter 3 kHz, resolution bandwidth 100 kHz, reference level −30 dBm

operating range and the highest locking frequency reported for any OPLL with semiconductor lasers.

2.3. OPLL Operation with Monolithically Integrated Photoreceiver. A *p-i-n*/HBT photoreceiver was substituted for the commercial photodiode. The InP-based HBT was grown by molecular beam epitaxy and consists of an $In_{0.53}Ga_{0.47}As$ base and collector regions and an $In_{0.52}Al_{0.48}As$ emitter layer. The photoreceiver circuit is shown in Figure 5. The −3-dB bandwidth of the circuit that was available for this experiment was 5.3 GHz, as measured with a lightwave test set (HP 83420A). The optical probe needed to direct the light onto the photoreceiver increased the optical path to about 3.4 ns, making the total loop delay approximately 5.3 ns. The gain of the photoreceiver as measured with the lightwave test set was 18 dB higher than that of the photodetector. However, difficulty in optimizing optical coupling when the *p-i-n*/HBT photoreceiver was inserted in the loop made the effective gain of the *p-i-n*/HBT photoreceiver only about 3 dB higher than that of the commercial photodiode used. The gain of the second LNA had to be decreased to compensate for the increased loop gain and to maintain stability. The additional gain available with improved alignment should allow for removal of one LNA with further optimization of the loop filter. Because of the higher gain, locking could be achieved well beyond the −3-dB point of 5.3 GHz, up to 7.5 GHz (approximately −9-dB point). With photoreceiver circuits of higher bandwidth and improved packaging techniques, this range is expected to reach the reported upper frequency limit of the integrated photoreceiver, that is, 19.5 GHz [10].

3. CONCLUSION

In conclusion, we have demonstrated the use of a fiber-based test bed OPLL with the use of semiconductor lasers. Our test bed demonstrates that in spite of the long loop delay associated with fiber-based components, a wide hold-in range (1.558 GHz) and a wide operating frequency range (1.00–20.75 GHz) could be achieved, both of which are among the best reported. Although our hybrid circuit is not an ideal OPLL for use in communications systems, it is more than adequate for use as a test bed for testing various components and/or their partial integrations. The combination of flexibility necessary to physically lay out various combinations of components and the excellent frequency range and locking range provide a stable environment for further work, and leads the way to a monolithically integrated OPLL.

We also demonstrated the use of a monolithically integrated *p-i-n*/HBT photoreceiver in an OPLL. The remaining transistor-based OPLL components are currently being designed with the use of the same transistor process used for the photoreceiver.

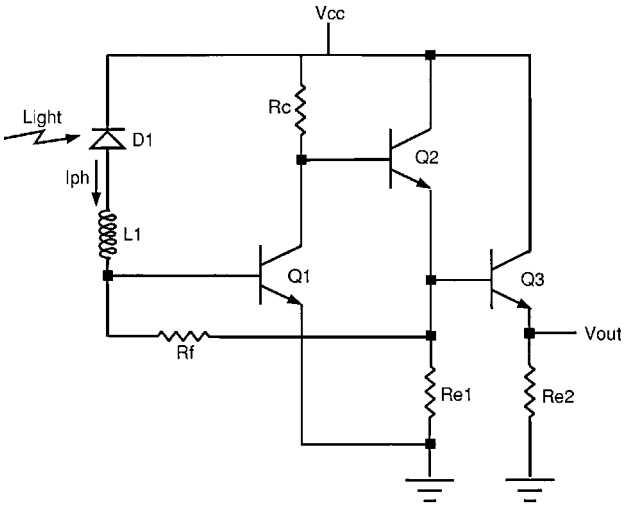

Figure 5 Circuit diagram of *p-i-n*/HBT photoreceiver

ACKNOWLEDGMENTS

The authors wish to thank U. Gliese and J. Keszenheimer for helpful discussions. The work is supported by the Army Research Office under the AASERT program (Grant No. DAAH04-95-1-0206). We would also like to thank Picometrix, Inc. for the use of their high-speed photodetector.

REFERENCES

1. R. J. S. Pedersen, U. Gliese, B. Broberg, and S. Nilsson, "Characterization of a 1.5 μm Three-Electrode DFB Laser," *Proc. 16th Eur. Conf. Opt. Commun. (ECOC '90—Amsterdam)*, The Netherlands, 1990, Vol. 1, pp. 279–282.
2. M. A. Grant, W. C. Michie, and M. J. Fletcher, "The Performance of Optical Phase-Locked Loops in the Presence of Non-negligible Loop Propagation Delay," *J. Lightwave Technol.*, Vol. LT-5, No. 4, 1987, pp. 592–597.
3. R. C. Steele, "Optical Phase-Locked Loop Using Semiconductor Laser Diodes," *Electron. Lett.*, Vol. 19, No. 2, 1983, pp. 69–71.
4. R. T. Ramos and A. J. Seeds, "Fast Heterodyne Optical Phase-Lock Loop Using Double Quantum Well Laser Diodes," *Electron. Lett.*, Vol. 28, No. 1, 1992, pp. 82–83.
5. U. Gliese, T. N. Nilsen, M. Bruun, E. L. Christensen, K. E. Stubkjaer, S. Lindgren, and B. Broberg, "A Wideband Heterodyne Optical Phase-Locked Loop for Generation of 3–18 GHz Microwave Carriers," *IEEE Photon. Technol. Lett.*, Vol. 4, No. 8, 1992, pp. 936–938.
6. M. Bruun, U. Gliese, T. N. Nielsen, A. K. Petersen, and K. E. Stubkjaer, "A 2 to 10 GHz GaAs MMIC Optoelectronic Detector for Optical Microwave Signal Generators," *Microwave J.*, Aug. 1994, pp. 94–100.
7. D. Trommer, R. Kaiser, R. Stenzel, and H. Heidrich, "Multi-Purpose Dual Tunable Laser/Combiner PIC Based on InP," *Proc. 21st Eur. Conf. Opt. Commun. (ECOC'95—Brussels)*, Mo.B.4.2, pp. 83–86.
8. A. L. Gutierrez-Aitken, K. Yang, X. Zhang, G. I. Haddad, P. Bhattacharya, and L. M. Lunardi, "16-GHz Bandwidth InAlAs-InGaAs Monolithically Integrated *p-i-n*/HBT Photoreceiver," *IEEE Photon. Technol. Lett.*, Vol. PTL-7, No. 11, Nov. 1995, pp. 1339–1341.
9. L. M. Lunardi, S. Chandrasekhar, A. H. Gnauck, C. A. Burrus, and R. A. Hamm, "20-Gb/s Monolithic *p-i-n*/HBT Photoreceiver Module for 1.55-μm Applications," *IEEE Photon. Technol. Lett.*, Vol. 7, No. 10, 1995, pp. 1201–1203.
10. K. Yang, A. L. Gutierrez-Aitken, X. Zhang, G. I. Haddad, and P. Bhattacharya, "Design, Modeling and Characterization of Monolithically Integrated InP-Based (1.55 μm) High-Speed (24 Gb/s) *p-i-n*/HBT Front-End Photoreceivers," *J. Lightwave Technol.*, Vol. 14, No. 8, 1996, pp. 1831–1839.
11. F. M. Gardner, *Phaselock Techniques* (2nd ed.), Wiley, New York, 1979, p. 17.
12. R. T. Ramos and A. J. Seeds, "Comparison between First-Order and Second-Order Optical Phase-Lock Loops," *IEEE Microwave Guided Wave Lett.*, Vol. 4, No. 1, 1994, pp. 6–8.

CCC 0895-2477/97